



Sharif University of Technology
Scientia Iranica
Transactions B: Mechanical Engineering
www.scientiairanica.com



Research Note

Visualization and analysis of nano-manipulation in liquid environment with atomic force microscopy

S. Esmailzadehha^a and M.H. Korayem^{b,*}

a. *Department of Mechatronics Engineering, Science and Research Branch, Islamic Azad University, Tehran, Iran.*

b. *Robotic Research Laboratory, Center of Excellence in Experimental Solid Mechanics and Dynamics, School of Mechanical Engineering, Iran University of Science and Technology, Tehran, Iran.*

Received 14 February 2013; received in revised form 14 December 2013; accepted 17 June 2014

KEYWORDS

Visualization;
Nano-manipulation;
Atomic force
microscopy;
Liquid forces.

Abstract. This paper focuses on theoretical analysis of AFM based nano-manipulation in a liquid environment. To achieve this goal, major forces in the liquid environment were reviewed and the manipulation processes were modelled by introducing the effect of intermolecular and hydrodynamic forces. The dynamic behaviour of pushing a gold nanoparticle of 50-nm radius on a silicon substrate at a velocity of 100 nm/s was investigated. A virtual reality user interface was also implemented and evaluated in a liquid environment, so users can get a sense of the forces. The results show that, in comparison to air, the required forces and time are increased by 2 and 6.5% for sliding and 2 and 4.3% for rolling in a liquid environment. Furthermore, for various submerged lengths of the cantilever in water, forces and time values are varied at 8 and 10.5%, respectively. Based on simulation results, sliding occurs at nominal values and critical forces and manipulation times in the liquid environment increase over the values. For biological manipulation purposes, the liquid environment is superior in comparison to air and the obtained results are verified by existing experiments.

© 2014 Sharif University of Technology. All rights reserved.

1. Introduction

AFM is an effective tool for studying molecular substrates [1]. AFM is a simple nano-manipulator used for nano-particles moving, riding on surfaces, cutting, perceiving, nicking, lifting and displacement. Figure 1 depicts the function of the AFM graphically.

Since a human operator cannot sense the nano-world directly, tele-operation between micro and macro systems in the nano-world [2] could be an alternative solution to forwarding perception to the operator. This operation is implemented in a virtual reality medium. Virtual reality is a medium for imagination, manipulation and contact with simulated environments. In

this paper, nano-manipulation in a liquid environment with forces applied on the cantilever tip is shown in a perceptible sense, graphically. These forces include horizontal and vertical cases.

Much research has been carried out on nano/micro manipulation in liquid environments. Savia et al. [3] proposed a numerical method to estimate adhesion forces. Mori showed that the adhesion force between a glass particle and a hydrophilic plate increases with relative humidity due to strong capillary condensation [4]. Theande et al. [5] performed force and friction measurements using atomic force microscopy and the colloidal probe technique in a liquid environment at different concentrations of sodium oleate. Drummond and Israelachvili [6] studied the wettability of rock surfaces. They measured the interactions between

*. *Corresponding author. Tel./Fax: +98 21 44865239;
E-mail address: hkorayem@iust.ac.ir (M.H. Korayem)*

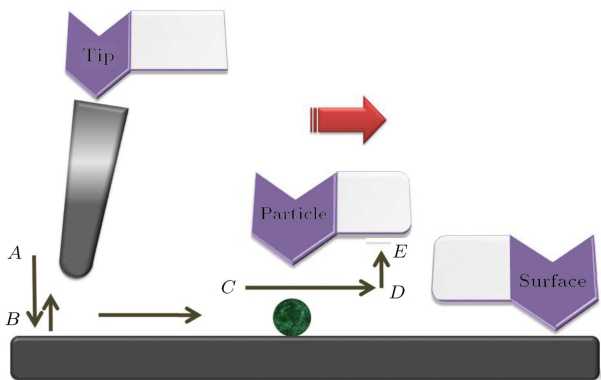


Figure 1. Manipulation using an AFM probe as a nano-manipulator.

different materials in contact and established their implications on the observed wetting behavior. Noy et al. [7] performed a comparison of measuring forces in ultra-high vacuums, liquids, and ambient air.

Butt [8] described the technique of AFM force measurement and analyzed force curves obtained under different conditions. Grierson and Flater [9] discussed nano-scale adhesion determination and friction properties between solids. Putman et al. [10] has shown that standard cantilevers can be used for tapping mode AFM in air, and successfully used a cantilever for the tapping mode AFM in liquid. Goryacheva and Makhovskaya [11] developed an analytical solution to analyze the influence of the adhesion interaction potential and volume of liquid. Lokar and Ducker [12], on the other hand, used a thermodynamic argument to predict the adhesion between two solid surfaces. Liang et al. [13] briefly reviewed the theories of the colloidal forces between particles and surfaces, including van der Waals forces, electrical double layer forces, salvation forces, hydrophobic forces and steric forces.

Luckham [14] gave examples of direct measurements of van der Waals, electrical double layer and steric forces, and showed how they can be modified and affect the properties of bulk suspensions. Carine et al. [15] developed a detailed theoretical model of the experimental setup, which accounts for surface forces, hydrodynamic interactions, droplet deformation, and AFM cantilever deflection. Jones [16] discussed and compared the interaction between cantilever, substrate and fluid, while generating force curves, and theoretical models for squeeze-film effects and drag on the SPM cantilevers were quantified. Bonaccorso [17] reviewed experimental work on confined Newtonian and non-Newtonian liquids using the AFM. Shen [18] presented a new understanding of adhesion and anti-adhesion of a liquid to a solid surface under dynamic conditions. The effect of disjoining pressure between a rigid spherical probe particle and a liquid interface was studied by Chan [19]. Resch [20] controlled manipulation of individual gold nano-particles in liquid environments

using the tip of a scanning force microscope for the first time, and Best [21] studied single-molecules, and compared them both, quantitatively and qualitatively, to those derived from conventional protein folding studies.

Seantier focused on AFM high resolution imaging of transmembrane proteins in model and native membranes [22]. Neto provided a review of experimental studies regarding the phenomenon of slip of Newtonian liquids at solid interfaces, and dedicated particular attention to effect factors such as surface roughness. Gauthier [23] presented an overview of the micro forces in air and liquid and then introduced a review of the major differences between dry and submerged micromanipulations. He gives an experimental analysis of the physical phenomena at a microscopic scale in dry and liquid media [24]. At this scale, the molecules of the water are not perceptible, whereas, by moving the probe in the nano-scale molecules, they become observable and can be followed graphically.

This paper is organized as follows. First, the forces in the liquid environment and the manipulation of nano-particles are modelled. Next, the manipulation of the nano-particles in liquid medium is visualized. Then, the results of simulation are analysed and discussed.

2. Nanomanipulation modelling in liquid medium

In this study, nano-particles with a radius of R_p are modelled. Particles are absorbed in the base plate and moved through the AFM probe under fluid conditions. Different steps are considered in nano-manipulation of the particle movement. Liquid forces are divided into two groups including intermolecular forces and hydrodynamic forces. Applied forces in the liquid environment have two forms; molecule reaction forces and macro forces. Intermolecular forces include surface tension, electrostatic double layer force, squeeze film force, solvation force, hydration force, steric force and adhesion force.

When the AFM probe is submerged in liquid, contact between the liquid surface and the cantilever occurs. The cantilever moves to push the particle, and the liquid surface stretches and resists movement. To overcome this effect, dW , which is proportional to the increase in surface area, dA [23], is applied. Introducing the proportional constant, γ , we have, in Eq. (1):

$$dw = \gamma.dA. \quad (1)$$

Constant γ is called surface tension, b is the perimeter of the cantilever and the force can be calculated in Eq. (2):

$$F = \frac{dW}{Dx} = -2\gamma b. \quad (2)$$

Since, the water is a high dielectric fluid, absorption and defusion of the charge in it is high. Ions and the surfaces with electrical charges make an electrical layer. When an opposite area (charge with both signs) is close to it, then ions will be increased among the layers and make a repulsing force. This force decreases at high distances, strongly [6]. The relation between the potentials and closing time is as follows: $\psi(\xi = x) = \psi_2$, $\psi(\xi = 0) = \psi_1$. The force rate is also defined as the following in Eq. (3):

$$F_{el}^{cp} = \frac{2\pi R \varepsilon \varepsilon_0}{\lambda_D} \left[2\psi_S \psi_T e^{-D/\lambda_D} - (\psi_S^2 + \psi_T^2) e^{-2D/\lambda_D} \right]. \quad (3)$$

Once the cantilever nears the surface, relative to its width, squeeze-film effects between the cantilever and substrate dominate the force response of the cantilever [16]. Suppose that there is a parallel beam with the surface, as $\varepsilon = W/L \ll 1$, and a dimensionless gap, $S = H/W \ll 1$, as the height. Then, flow equations will be in stock form under a thin layer, and the obtained force is in Eq. (4):

$$F_S = \mu V L \left(\frac{1}{S} \right)^3. \quad (4)$$

It is applied to the whole of the cantilever. The force of the squeeze film loses its effect as the distance increases.

A fluid structure close to the wall has a distinct property in volume shape. Most fluids have differed normal densities near the wall, for which the period of this vibration or frequency is equal to the diagonal of the fluid molecules. This region develops for several molecule distances and makes a frequent or vibrating force, in a pulse-repulsive state. Molecules settle in different layers in this distance. Density fluctuations and specific interactions cause an exponentially decaying oscillatory force. The period of the oscillations corresponds to the thickness of each layer. Such forces are entitled solvation forces, because they are a consequence of the adsorption of solvent molecules to solid surfaces [8].

Solvation forces are often well described by an exponentially decaying oscillating function of the form of Eq. (5):

$$f = f \cos \left(\frac{2\pi x}{\sigma} \right) e^{-x/\lambda}. \quad (5)$$

Hydration is another force in this environment. Under the hydration effect of two areas, considering a continuous fluid environment, there is a force from 1 to 3 nano-Newtonian, as repulsive, in areas where the fluid diagonal is less than the fluid molecules. In fact, this force is a kind of short range force with a small density of salt less than 0.1 M/Lit and, so, it is negligible compared to the electrostatic force. In

some cases, in smooth areas and low salty densities, this force decreases at high distances exponentially and the repulsive energy rate is estimated as Eq. (6):

$$U = A e^{-X/\lambda_H}. \quad (6)$$

λ_H is decay length, and amplitude A is equal to 0.001–10 J/m³. This force has a higher contribution at high densities compared to the electrostatic force.

Another force is Steric Force or a force in the mean of the atomic arrangement force in space. This force is usually made by a repulsive form between two covered areas, with polymer, in a suitable solution. Polymer molecules under adhesive power in the area make a repulsive force with increasing entropy as a result of hanging the chains into the area when the molecules are close to each other. Eqs. (7) and (8) formulate this force:

$$L_0 = n l^{5/3} \Gamma^{1/3}, \quad (7)$$

$$f(x) = K_B T \Gamma^{3/2} \left[\left(\frac{2L_0}{x} \right)^{9/4} - \left(\frac{x}{2L_0} \right)^{3/4} \right]. \quad (8)$$

Perhaps adhesion force is one of the most important forces in nano views. This force is made as a result of probe contact with the sample and enough energy is required for separation in this case. Owing to more complexity in adhesive power, many studies have reported on these nano-forces. It is often believed that this force is a combination of electrostatic force, Vander valence, chemical bonds, acid and base. Such a combination is implemented here as adhesive energy in the area, and the Johnson-Kendall-Roberts theory in contact dynamics is calculated. The area adhesive energy between the nano-particles and the probe is supposed as $w = 0.2 \text{ J/m}^2$ in the JKR model (a rational rate for the areas in a fluidity state) [7,8].

$$\omega = \frac{H}{24\pi D_o}. \quad (9)$$

Lastly, another force is the hydrophobic force, by which, escaped water areas absorb each other strongly. This is water escaped force and it occurs on surfaces with a contact angle of more than 90 degrees. This event does not occur at all when one of the areas is related to the escaped ones, and the other one is adopted with water.

Drummond and Israelachvili [6] showed that the reaction between two areas in the escaped water property is stronger than the Vander valence force. Although there are many studies related to this field, there is no obvious evident and calculative theory in practice. It seems that this force has a short term for distances at 2-6 nm and a long term at until 100 nm distances.

One of the main forces in macro aspects is drag force. It is the result of fluid movement on cantilever areas. There are two kinds of drag by fluid movement:

1. Pushing drag in vertical areas on fluid flow (it is negligible due to very low thickness of the cantilever);
2. Frictional drag as a result of fluid movement on both sides (up and down) and tensile shear.

There are different methods for estimation of the drag coefficient. Many researchers have considered the AFM cantilever as a cylinder shape [24] and studied the drag force of the cantilever form, as well.

In recent modelling methods, the cantilever moves in a horizontal path and parallel with the base plate. Because of the small and thin thickness of the cantilever compared to the width and length and low Reynolds of the flow, the drag coefficient rate is the same as the drag coefficient in a rectangular cube. So, frictional drag inserts in two sides. Suppose that C_D is in Eq. (10):

$$C_D = \frac{8\pi}{Re_D \log\left(\frac{7.4}{Re_D}\right)}. \tag{10}$$

Drag force from the fluid is in the form of Eq. (11):

$$F_{Drag} = C_D \frac{1}{2} \rho V^2 (DL). \tag{11}$$

In fact, frictional drag force is applied on up and down areas of the cantilever and focused on it, extremely. Jump flow is considered a flow with low Reynolds rate, and a fluid with a non-compressibility state. When the cantilever is submerged in liquid, due to the flow

passing above and below the object, there are drag effects on both sides.

In order to derive the drag force, the velocity profile should be calculated. In this study, we investigate steady flows at low Reynolds number, restricting ourselves to incompressible flows. The equation of motion is expressed in the form of Eq. (12):

$$F_{D_{Top}} = WL \left(\frac{3\mu^2 U}{H^2} - \frac{6\mu U}{H^3} \left(H - \frac{h}{2} \right) \right) \left(y + \frac{2\mu U}{H \frac{\partial p}{\partial x}} - H \right). \tag{12}$$

Below the cantilever, there are forces according to Eq. (13):

$$\text{Assume } \left(\frac{\partial p}{\partial x} \right) = 0 \Rightarrow F_{D_{Below}} = WL\mu \frac{U}{h}. \tag{13}$$

3. Dynamic modelling of nanomanipulation process in liquid environment

Figure 2 illustrates all the forces that are applied on top of the cantilever. In the nano-manipulation process, the probe is considered as a cylinder shape. The forces, probe and cantilever, as well as the contact force between the particle and the probe or the cantilever and the probe can be observed in Figure 2. In these figures, the forces are shown in two different views, $y-z$ and $x-z$, where F_y and F_z are horizontal and vertical components between the cantilever and probe. F_T is a contact force between the probe and the particle.

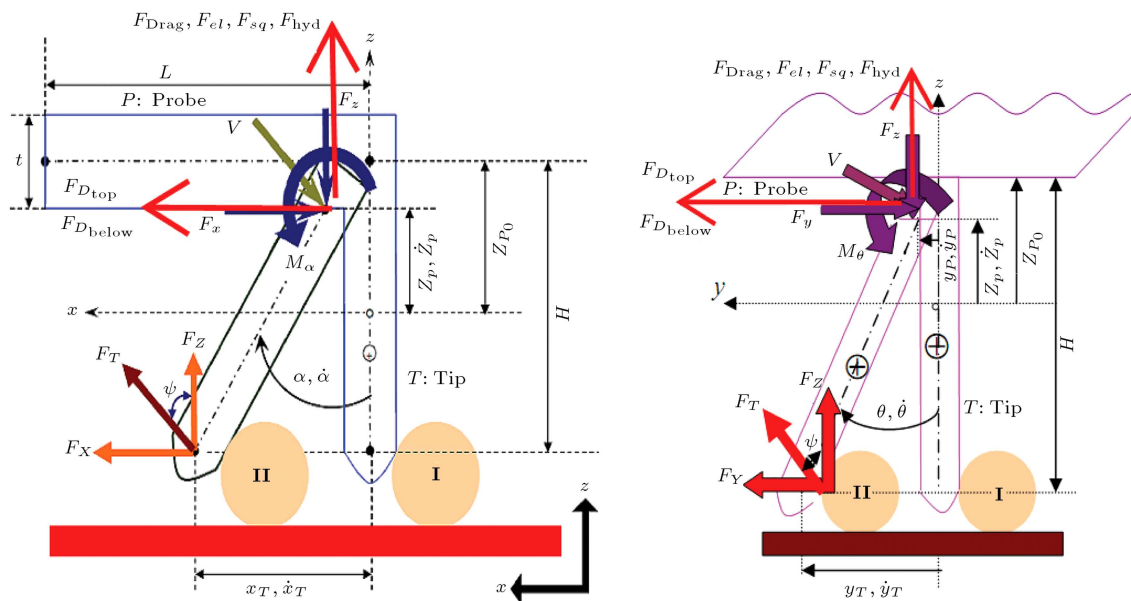


Figure 2. a) AFM cantilever and probe bending along $y-z$ axes during pushing nano objects [2]. b) AFM cantilever and probe bending along $x-z$ axes during pushing nano objects.

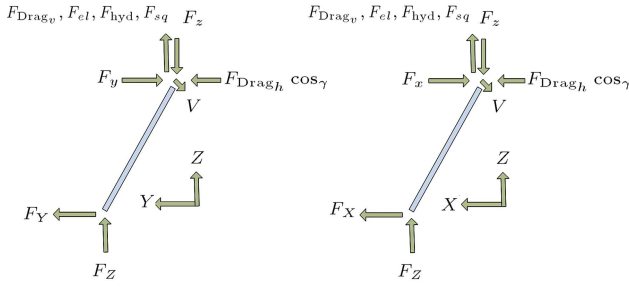


Figure 3. FOB of probe.

Dynamic equations are developed based on the free body diagram (FOB) of a pushing system, including the AFM cantilever and probe, nanoparticle and substrate. Figure 3 presents the FOB of the probe of the AFM in contact with the particle.

The kinematic equations of the cantilever can be written in the form of Eq. (14):

$$\begin{aligned}
 z_p &= z_{afm} + H \cos(\theta) \cos(\alpha) + (R_p - \delta_s) \\
 &\quad + (R_t + R_p - \delta_t) \cos(\varphi), \\
 x_p &= x_{afm} - (R_t + R_p - \delta_t) \sin(\varphi) - H \sin(\alpha), \\
 y_p &= y_{afm} - (R_t + R_p - \delta_t) \sin(\varphi) - H \sin(\theta). \quad (14)
 \end{aligned}$$

In dynamic equations, movement is along X , Y and Z directions and momentum is estimated by balance Eqs. (15)-(18). z_p , x_p , y_p are obtained by differentiation from equations, then, a final rate of F_y , F_x and F_z can be calculated:

$$\begin{aligned}
 \sum \vec{F}_y &= m\vec{a}_y \Rightarrow F_Y + (F_{D_{top}} + F_{D_{below}}) \cos \gamma \\
 &\quad - F_y - V \cos \theta = m \left(\frac{\ddot{y}_T + \ddot{y}_p}{2} \right), \quad (15)
 \end{aligned}$$

$$\begin{aligned}
 \sum \vec{F}_x &= m\vec{a}_x \Rightarrow F_X + (F_{D_{top}} + F_{D_{below}}) \sin \gamma \\
 &\quad - F_x - V \cos \alpha = m \left(\frac{\ddot{x}_T + \ddot{x}_p}{2} \right), \quad (16)
 \end{aligned}$$

$$\begin{aligned}
 \sum \vec{F}_z &= m\vec{a}_z \Rightarrow F_Z + (F_{Drag} + F_{el} + F_{sq} + F_{hyd}) \\
 &\quad - F_z - V \sin \theta - V \sin \alpha = m \left(\frac{\ddot{z}_T + \ddot{z}_p}{2} \right), \quad (17)
 \end{aligned}$$

$$\begin{aligned}
 \sum \vec{M}_p &= I_p (\ddot{\theta} + \ddot{\alpha}) \Rightarrow M_\theta + F_z H \sin \theta \sin \alpha \\
 &\quad - F_Y H \cos \theta - M_\alpha - F_x H \cos \alpha = I_p (\ddot{\theta} + \ddot{\alpha}). \quad (18)
 \end{aligned}$$

Finally, pushing force, F_T and ψ , can be calculated

from the following Eqs. (19)-(21):

$$F_{XY} = \sqrt{F_X^2 + F_Y^2}, \quad (19)$$

$$F_T = \sqrt{F_{XY}^2 + F_Z^2}, \quad (20)$$

$$\psi = \tan^{-1} \left(\frac{F_Y}{F_Z} \right). \quad (21)$$

Friction and normal forces are defined for a semi-static state, based on the probe angle and force, as in the following Eqs. (22):

$$\begin{aligned}
 f_t &= F_T \cos \zeta, & F_t &= -F_{T_{tip}} \sin \zeta, \\
 f_s &= F_T \cos \psi - F_{DP}, & F_s &= -F_{T_{sub}} \sin \psi. \quad (22)
 \end{aligned}$$

F_t is the sliding friction force on the probe tip and base plate, and f_s is the friction on the real contact area and vertical force. So, the frictional model for sliding and rolling is defined in the following equations:

$$F_T > \frac{F_{DP} + \tau_s A_s}{\sin \psi - \mu_s \cos \psi}, \quad (23)$$

$$F_T > \frac{F_{DP} R + \tau_{rs} A_s + \tau_{rt} A_t}{R_P (\sin \psi + \cos \xi) + \mu_{rt} \sin \xi - \mu_{rs} \cos \psi}. \quad (24)$$

In the above equations, μ is friction ratio, τ is shear stability and A is contact area between the particle and base plate. Critical force, F_T depends on the particle moving angle, G , the probe and particle contact angle, frictional constants, contact area, and applied dragging force, on the particle at all times.

4. Simulation of virtual reality environment

Dynamic modeling results in understanding the pushing procedure in real time. Therefore, by modelling all the forces and dynamics of the particles, nano-particles can be traced momentarily and located at the desired positions [25].

In the nano-manipulation scheme, there are two methods for pushing as follows:

1. The substrate moves the targeted particles;
2. The tip moves and displaces the nano-particle.

In this research, it was assumed that the tip moves and displaces the nano-particle. Values that are used in this study are according to the simulation data of Sitti and Tafazoli [26]. Using the same data, Korayem et al., in [27], has compared the findings of his simulation with previous findings. In this simulation, a gold particle with $R_p = 50$ nm has been pushed onto the silicon oxide substrate that moves with constant

Table 1. The AFM geometric constants.

d (μm)	L (μm)	W (μm)	t (μm)	H (μm)	R_p (μm)
4	225	48	1	12	20

Table 2. Tribological parameters between tip/nano particle and nano particle/substrate.

μ_s	μ_d	μ_r	τ	τ_r
0.8	0.7	80 nm	28 MPa	28 Pa.m

Table 3. AFM mechanical properties.

E (GPa)	ν	G (GPa)	ρ (kg/m^3)
169	0.27	66.54	2.330

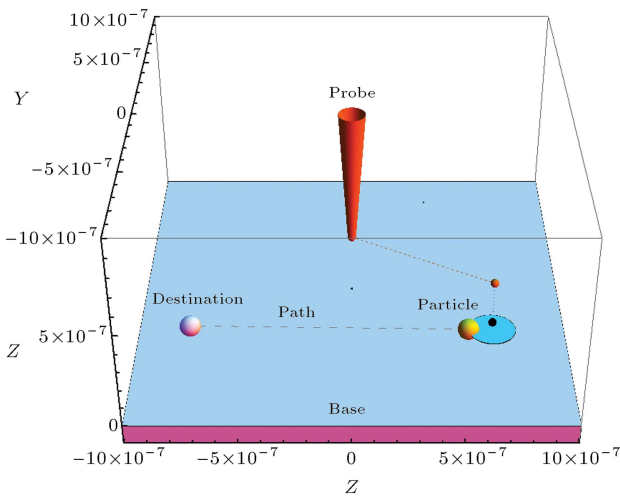


Figure 4. Virtual reality environment.

velocity. Geometrical and mechanical properties of the RC are summarized in Tables 1, 2 and 3 [26].

The base plate is in the form of a rectangular cube with the following dimensions: $(X, Y, Z) = (2000, 2000, 100)$. The scope of movement for the tip of the AFM probe along X and Y is from -1000 to $+1000$, and along Z, from 0 to $+1000$. The primary position for the tip of the probe is $(0, 0, h)$ [28].

Nano-particles with a default radius of $R_p = 50$ nm are placed on the base plate. The tip of the cantilever probe is shown as a red cone, with a radius of $R_{tip} = 20$ nm. The position of the atoms should be specified by the user who should first enter the number of the desired atom in the graphical interface of the written software. Then, final coordinates for manipulation have to be determined, which is set through a slippery band. With the aid of this band, the user can handle X or Y coordinates separately so that the other one remains unchanged. While using the graphical window, the user can simultaneously observe the final result dynamically.

Figure 4 shows that the desired atom should

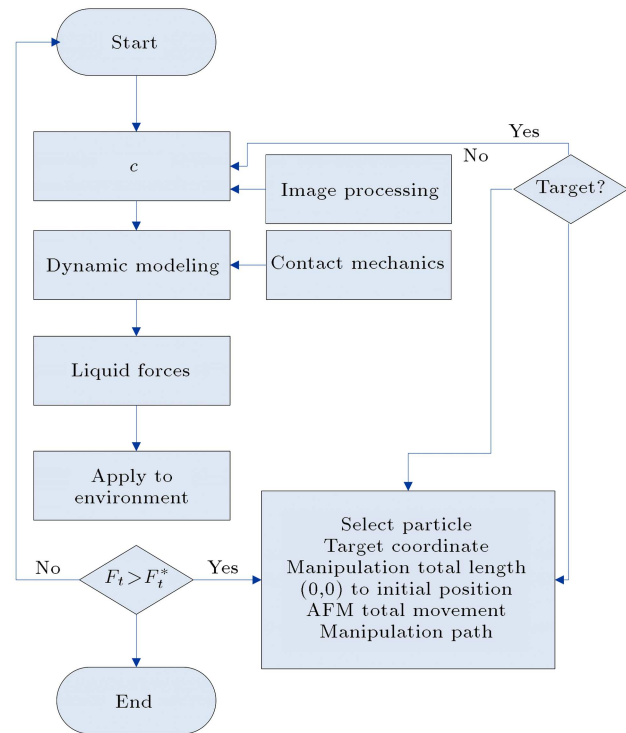


Figure 5. Flowchart of virtual reality environment.

be selected for manipulation. After selecting the atom, the destination coordinate has to be inserted for manipulation.

The tip of the AFM probe has a safe height, called h_{safe} . This height prevents the tip from being hit or damaged by atoms or other physical obstacles when it moves toward the aimed nano-particle. In this program, it is assumed that one particle which has been chosen by the user is on the base plate, or at least there is no other atom or physical obstacle to the chosen method. An operational flowchart of the virtual reality environment is shown in Figure 5.

Liquid forces are applied to the tip of the cantilever. At first, the solvation force and then pushing forces are applied. In the solvation process, the probe has been surrounded by water molecules. In Figure 6, the drag force on the cantilever is displayed separately. As shown in Figure 7, the electrostatic force is based on the compacting effect and increases by closing the layer.

4.1. Manipulation of nanoparticle

For manipulating nano-particles with the AFM in contact mode, the whole operation should be divided into sections, and each section should be studied separately. In Figure 8, different stages of pushing the nano-particle are shown and are reported below.

In the nano-manipulation process, the cantilever moves from the origin to the nano-article coordinates. The probe and cantilever move in the air and reach the proper location. Then, the probe and cantilever come

down, get into the water and contact the base. Effective forces are shown in Figure 9. During movement, the probe and cantilever speed is constant.

Liquid forces are applied to the probe and cantilever. The probe has been surrounded by water molecules. Figure 9 illustrates electrostatic force based on a compacting effect, which is increased gradually.

In the parking stage, the probe contacts the area and the height is increased until a defined height. Figure 10 shows that the nano-particle is pushed and directed to the destination location. The

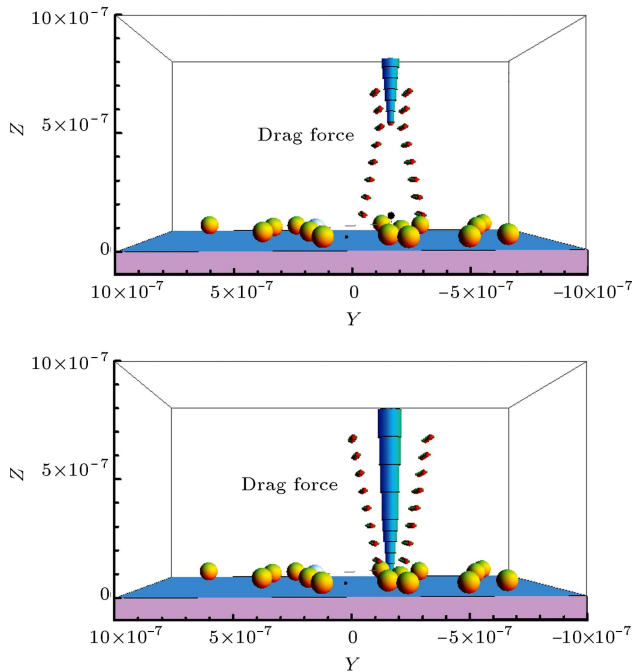


Figure 6. Applying the F -drag force.

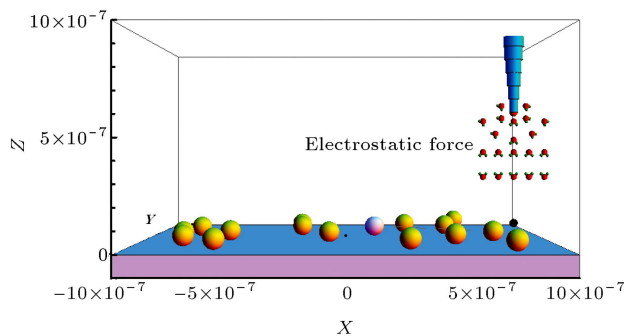


Figure 7. Create and eliminate electrostatic layers and squeeze file effect layer.

liquid forces are applied to the cantilever and the probe.

The cantilever and the probe get back to their original position. The solvation force is applied when the probe is separated from the nano-particle. Then, electrostatic and squeeze film forces are applied, as shown in Figure 11. The probe is moving away from the

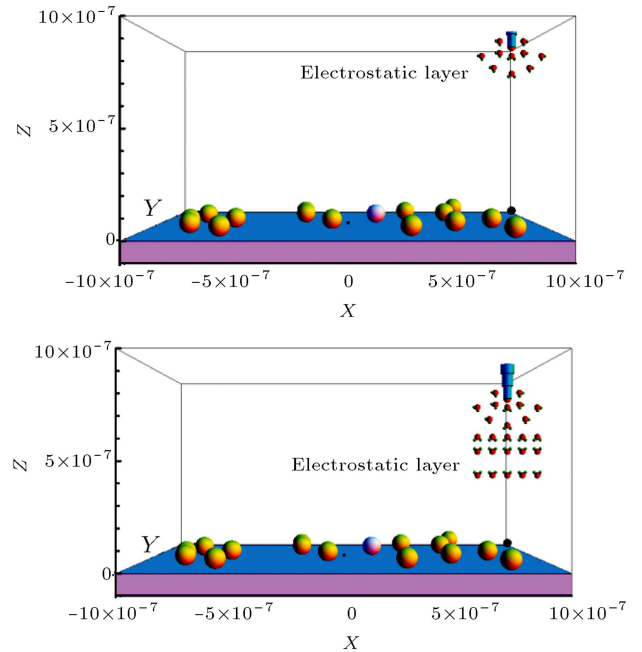


Figure 9. Gathering the water molecules of probe and cantilever and creation of electrostatic layers.

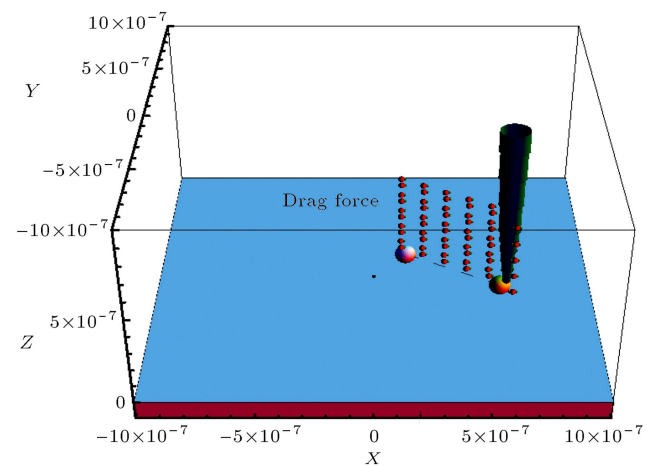


Figure 10. Applying the F -drag force to cantilever horizontally to push the particle.

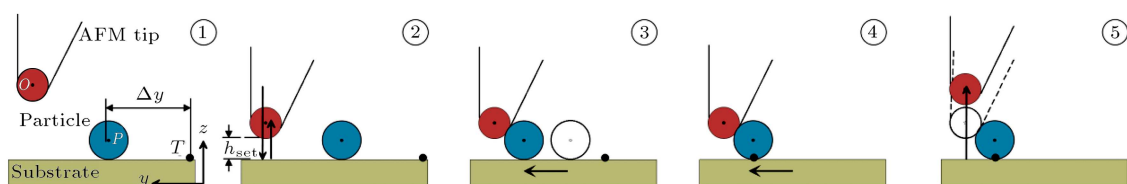


Figure 8. Manipulation of nanoparticle [2].

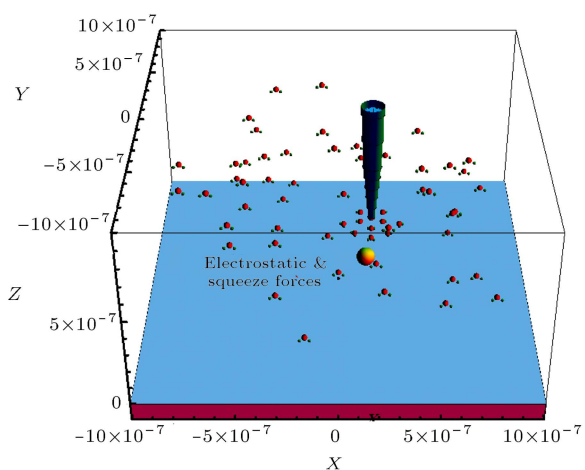


Figure 11. Applying electrostatic and squeeze file effect to cantilever.

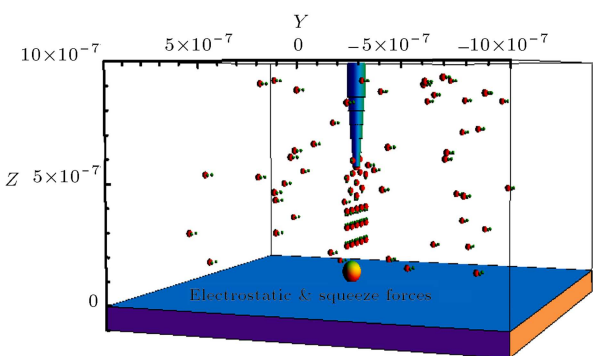
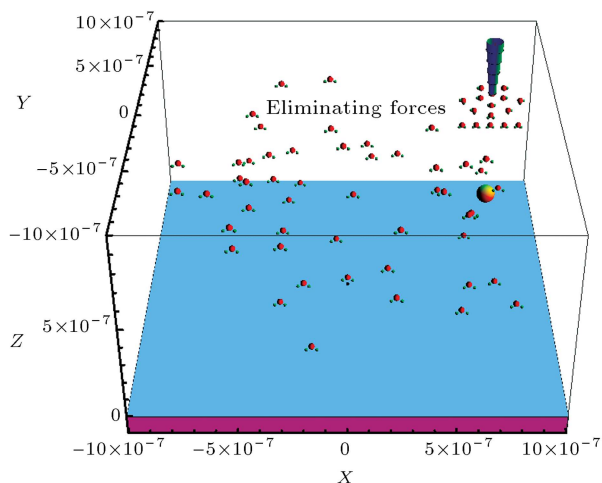


Figure 12. Probe goes away from surface base and eliminates electrostatic and squeeze file effect and hydration forces.



surface base and the electrostatic and squeeze file effect and hydration force were eliminated near the water surface in Figure 12.

5. Results and discussion

Applying liquid forces on virtual reality environments, we can observe the results of the manipulation process

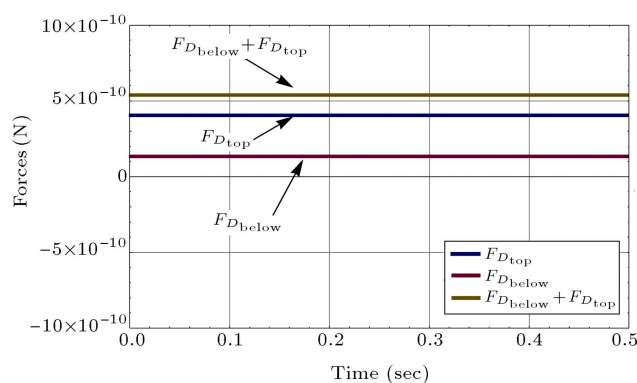


Figure 13. Below and top drag forces.

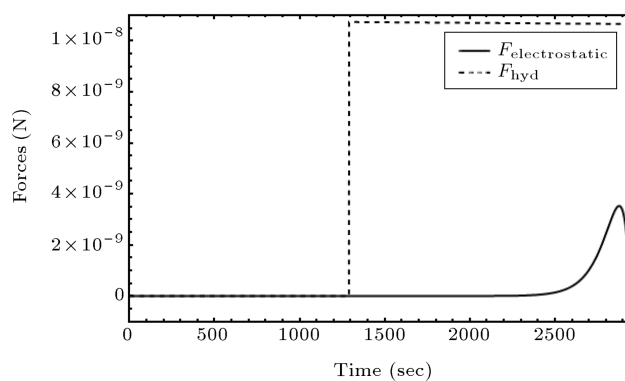


Figure 14. Electrostatic and hydration forces.

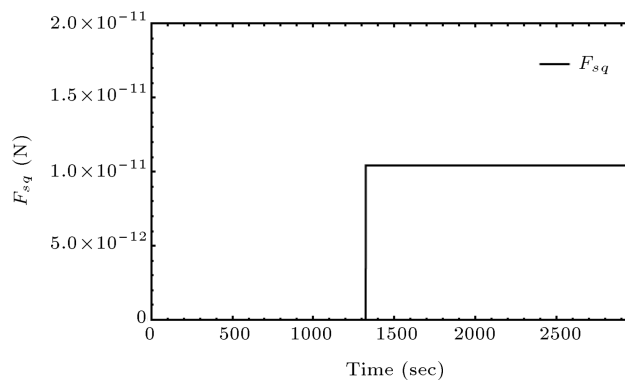


Figure 15. Squeeze effect force.

and see the effects of liquid forces. In Figure 13 the effect of $F_{D_{top}}$ and $F_{D_{below}}$ are shown. Figure 14 also depicts electrostatic and hydration forces. Squeeze and surface forces are shown in Figures 15 and 16, respectively.

Diagrams of F_T , F_s^* and F_r^* are plotted in Figure 17. It is shown that the intersection of F_T and F_s^*F diagrams occurs at $t = 0.142$ s, and a pushing force of $0.620 \mu\text{N}$. The intersection of F_T and F_r^*F diagrams occurs at $t = 0.162$ s, and a pushing force of $0.675 \mu\text{N}$. So, the nano-particle begins to slide before it rolls.

Rolling force for various submerged lengths of a cantilever in water is simulated. Four points are chosen and the cantilever is considered to be submerged in

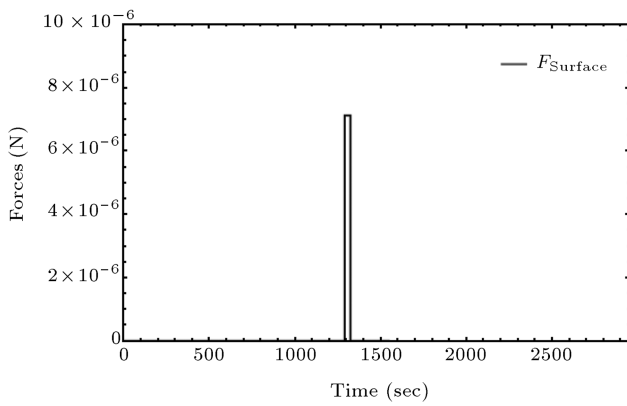


Figure 16. Surface force.

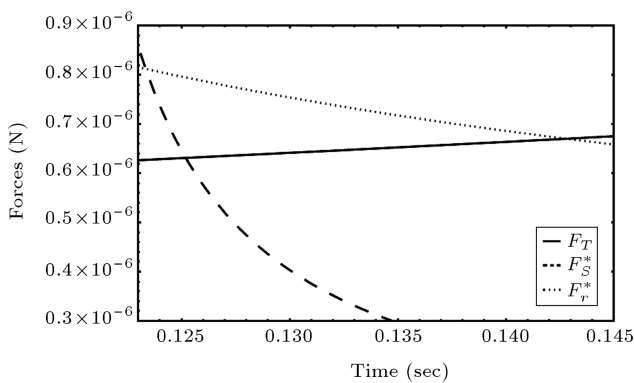


Figure 17. The intersection of F_T , F_s and F_r diagrams.

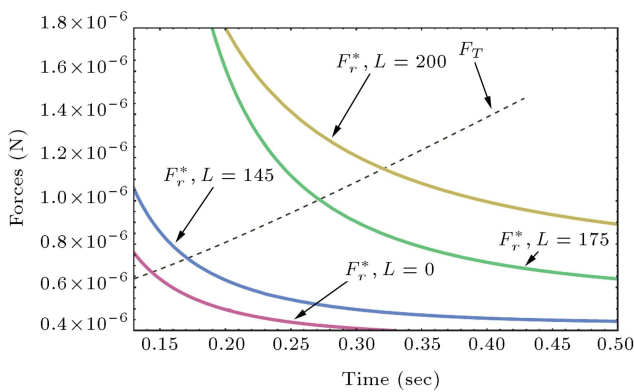


Figure 18. The intersection of F_T and F_r diagrams for various submerged lengths of cantilever in water.

water up to those points ($L = 0, 145, 175$ and $200 \mu\text{m}$). The results are shown in Figure 18 for the rolling force of the nano particle.

Figure 19 illustrates the intersection of the sliding force of nano-particles with F_T in an air environment. The intersection of F_T and F_s diagrams occurs at $t = 0.134$ s and a pushing force of $0.643 \mu\text{N}$.

In Figure 20, the intersection of the sliding force of nano-particles with F_T in a liquid environment is shown. The intersection of F_T and F_s diagrams occurs at $t = 0.180$ s and the pushing force of $0.655 \mu\text{N}$ in the liquid environment.

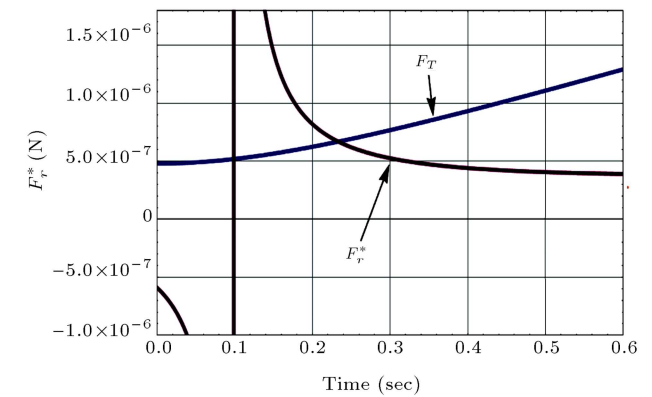
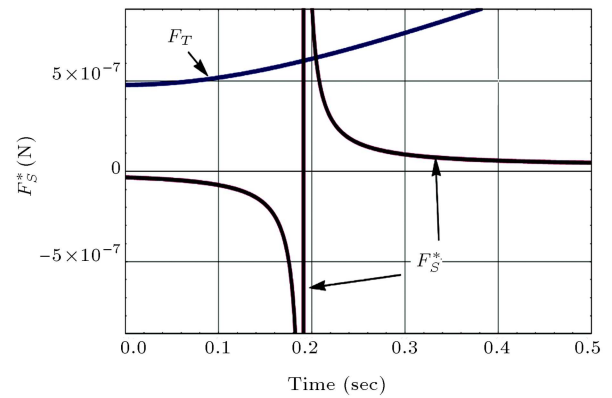


Figure 19. The intersection of F_T , F_s and F_r diagrams in air.

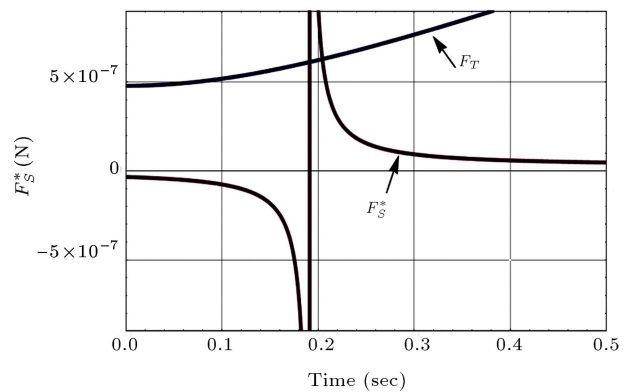
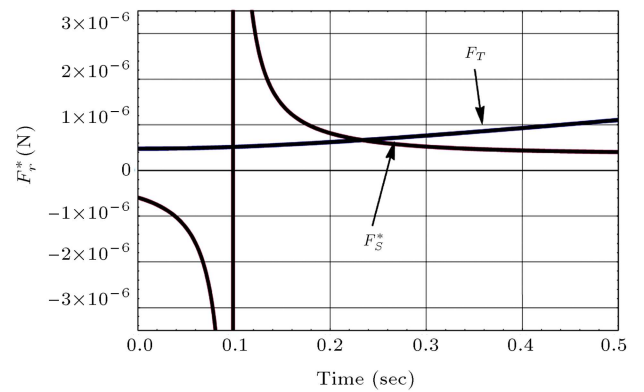


Figure 20. The intersection of F_T , F_s and F_r diagrams in liquid environment.

The intersection of F_T and F_r diagrams in the air environment occurs at $t = 0.152$ s and a pushing force of $0.681 \mu\text{N}$, while the intersection of F_T and F_r diagrams in a liquid environment occurs at $t = 0.203$ s and a pushing force of $0.692 \mu\text{N}$. The results show that sliding and rolling forces in the liquid environment have increased by 2% compared to air.

6. Conclusions

In this paper, forces in a liquid environment were reviewed, and manipulation processes, i.e. pushing a gold nano-particle, were studied by investigating their dynamic behaviour. By use of the nano-particle body diagram and modelling different forces, it became possible to determine the exact movement time of the nano-particle, the exact places of the nano-particle and probe tip at any time during pushing. A virtual reality medium for AFM based nano-manipulation in a liquid environment was developed and the manipulation process was simulated for nano-particles in a liquid environment. The exact place of the nano-particle was determined through inserting movement information in the VR environment. The effects of different submerged lengths of the cantilever have been simulated in this study and also the pushing time for a nano-particle was obtained.

It is concluded that a liquid environment can be used as an appropriate environment for the manipulation process. However, for an accurate nano-manipulation in a liquid environment, more studies and consideration of various intermolecular forces are needed. Results show that sliding forces in a liquid environment have been increased by 2% compared to the air, and the drag force has a smaller effect on the deflection of the cantilever than the surface tension [27]. It was obtained that the difference between the manipulation forces in air and water is not so reasonable, as mentioned in [19]. Liquid environments are suitable for the prevention of unwanted probe or particle movements, a fact that has been verified by Gauthier [23]. Nano-manipulation in liquid environments can be used for different applications in sciences, such as medicine and chemistry, which should be further considered.

References

1. Fotiadis, D., Scheuring, S., Muller, S., Engel, A. and Muller, D.J. "Imaging and manipulation of biological structures with the AFM", *J. of Micron*, **33**, p. 385 (2002).
2. Sitti, M. "Teleoperated 2-d micro/nano manipulation using atomic force microscope", PhD. Dissertation, University of Tokyo, Tokyo, Japan (1999).
3. Savia, M., Koivo, H.N. and Zhou, Q. "Evaluation of adhesion forces between arbitrary objects", *J. of Micromech.*, **3**, pp. 221-238 (2006).
4. Mori, Y. "Effect of surface hydrophobicity on interaction between particle and flat plate at final stage of wet coating process", *J. of Colloids and Surfaces A: Physicochemical and Engineering Aspects*, **311**, pp. 61-66 (2007).
5. Theander, K., Pugh, R.J. and Rutland, M.W. "Forces and friction between hydrophilic and hydrophobic surfaces: Influence of oleate species", *J. of Colloid Interface Sci.*, **313**(2), pp. 735-46 (2007).
6. Drummond, C. and Israelachvili, J. "Surface forces and wettability", *J. of Petroleum Sci. and Eng.*, **33**, pp. 123-133 (2002).
7. Noy, A., Frisbie, C.D., Rosznyai, L.F., Wrighton, M.S. and Lieber, C.M. "Chemical force microscopy: Exploiting chemically modified tips to quantify adhesion, friction and functional group distributions in molecular assemblies", *J. of Am. Chem. Soc.*, **117**, pp. 7943-7951 (1995).
8. Butt, H. "Force measurements with the atomic force microscope: Technique, interpretation and applications", *J. of Surface Sci. Reports*, **59**, pp. 1-152 (2005).
9. Grierson, D.S. and Flater, F. "Accounting for the JKR-DMT transition in adhesion and friction measurements with AFM", *J. of Adhesion Sci. Tech.*, **19**, pp. 291-311 (2005).
10. Putman, A.J., Werf, O.W. and Degrooth, G. "Tapping mode atomic force microscopy in liquid", *J. of Appl. Phys. Lett.*, **64**, pp. 2454-2456 (1994).
11. Goryacheva, I. and Makhovskaya, Y. "Adhesion effects in contact interaction of solids", *J. of Mecanique*, **336**, pp. 118-125 (2008).
12. Lokar, W.J. and Ducker, W.A. "Approximate prediction of adhesion between two solids immersed in surfactant solution based on adsorption to an isolated solid", *J. of Colloids and Surfaces A: Physicochemical and Engineering Aspects*, **332**, pp. 256-260 (2008).
13. Liang, Y., Hilal, N., Langston, P. and Starov, V. "Interaction forces between colloidal particles in liquid: Theory and experiment", *J. of Advances in Colloid and Interface Science*, **135**, pp. 151-166 (2007).
14. Luckham, P.F. "Manipulation forces between surfaces: applications in colloid science and biophysics", *J. of Advances in Colloid and Interface Science*, **111**, pp. 29-47 (2004).
15. Carine, L., Chan, Y.C. and Lewis, C. "Measurement of dynamical forces between deformable drops using the AFM", *J. of Langmuir*, **21**, pp. 2912-2922 (2005).
16. Jones, R.E. and Hart, D.P. "Force interactions between substrates and SPM cantilevers immersed in liquids", *J. of Tribol., Int.*, **38**, pp. 355-361 (2005).
17. Bonaccorso, E. "Thin liquid films studied by atomic force microscopy", *J. of Current Opinion in Colloid & Interface Science*, **13**, pp. 107-119 (2007).

18. Chan, D. "Forces between a rigid probe particle and a liquid interface", *J. of Colloid and Interface Sci.*, **236**, pp. 141-154 (2000).
19. Resch, R., Lewis, D., Meltzer, S. and Montoya, N. "Manipulation of gold nanoparticles in liquid environments using SFM", *J. of Ultramicroscopy*, **82**, pp. 135-139 (1999).
20. Seantier, B. "Probing supported model and native membranes using AFM", *J. of Current Opinion in Colloid & Interface Science*, **13**, pp. 326-337 (2008).
21. Gauthier, M. "PRONOMIA project: Micro-assembly and modeling of the microworld", *Int. Conf. on Intelligent Robotics and Systems*, San Diego (2007).
22. Dyson, P., Ransing, R.S., Williams, P.M. and Williams, P.R. "Fluid properties at nano/meso scale: A numerical treatment", In *Microsystem and Nanotechnology*, Wiley (2008).
23. Korayem, M.H. and Esmaeilzadehha, S. "Virtual reality interface for nano-manipulation based on enhanced images", *Int. J. of Advanced Manufacturing Technology*, **63**, pp. 1153-1166 (2012).
24. Sitti, M. and Tafazzoli, A. "Dynamic behavior and simulation of nanoparticle sliding during nanoprobe-based positioning", *ASME Int. Mech. Eng. Congress*, pp. 965-972 (2004).
25. Korayem, M.H., Motaghi, A. and Zakeri, M. "Dynamic modeling of submerged nanoparticle pushing based on atomic force microscopy in liquid medium", *J. of Nanoparticle Research*, **13**, pp. 5009-5019 (2011).
26. Korayem, M.H., Esmaeilzadehha, S., Rahmani, N. and Shahkarami, M. "Nano manipulation with rectangular cantilever of atomic force microscope in a virtual reality environment", *Digest J. of Nanomaterials and Biostructures*, **7**, pp. 435-445 (2012).
27. Shen, W. "Adhesion and anti-adhesion of viscous fluids on solid surfaces - A study of ink transfer mechanism in waterless offset printing", *J. of Colloid and Interface Science*, **318**, pp. 348-357 (2007).
28. Best, B., Brockwell, D. and Toca, L. "Force mode atomic force microscopy as a tool for protein folding studies", *J. of Analytica Chimica Acta*, **479**, pp. 87-105 (2003).

Biographies

Soliman Esmaeilzadehha was born in Qazvin, Iran, in 1981. He received BS (Electrical Engineering) and MS (Mechatronics) degrees from Azad University, Iran, in 2003 and 2006, respectively, and is currently a PhD degree candidate at the same institute in the field of Mechatronics. His research interests include robotic systems, atomic force microscopy dynamics, sensitivity analysis, and nano-technology.

Moharam Habibnejad Korayem was born in Tehran, Iran, in 1961. He received his BS (Hon) and MS degrees in Mechanical Engineering from Amirkabir University of Technology, Tehran, Iran, in 1985 and 1987, respectively and a PhD degree in Mechanical Engineering from the University of Wollongong, Australia, in 1994. He is currently Professor of Mechanical Engineering at Iran University of Science and Technology, where he has been involved for the last 17 years in teaching and research activities in the area of robotics. His research interests include the dynamics of elastic mechanical manipulators, trajectory optimization, symbolic modelling, robotic multimedia software, mobile robots, industrial robotics standard, robot vision, soccer robot, and analysis of mechanical manipulators with maximum load carrying capacity. Dr. Habibnejad Korayem has published more than 470 papers in international journals and conferences in these areas.